



ARCHIVES  
of  
FOUNDRY ENGINEERING

ISSN (2299-2944)  
Volume 2023  
Issue 4/2023

169 – 172

20/4



10.24425/afe.2023.148960

Published quarterly as the organ of the Foundry Commission of the Polish Academy of Sciences

# Microstructure and Properties of Experimental Mg-9Al-5RE-1Zn-Mn Magnesium Alloy

K. Braszczyńska-Malik 

Czestochowa University of Technology, Faculty of Production Engineering and Materials Technology, Department of Materials Engineering, 19 Armii Krajowej Ave., 42-200 Czestochowa, Poland

Corresponding author: E-mail address: k.braszczyńska-malik@pcz.pl; kacha@wip.pcz.pl

Received 04.09.2023; accepted in revised form 11.12.2023; available online 29.12.2023

## Abstract

In this paper, an experimental Mg-Al-RE-type magnesium alloy, named AEZ951, is presented. The chemical composition of the investigated alloy was ca. 9 wt% Al, 5 wt% RE (rare earth elements), 0.7 wt% Zn and 3 wt% Mn. The experimental material was gravity cast into a cold steel mould. Microstructure analyses were carried out by light microscopy, along with X-ray phase analysis and scanning electron microscopy with an energy-dispersive X-ray spectrometer (SEM + EDX). Detailed investigations disclosed the presence of primary dendrites of an  $\alpha$ (Mg) solid solution and  $Al_{11}RE_3$ ,  $\gamma$  and  $Al_{10}RE_2Mn_7$  intermetallic compounds in the alloy microstructure. The volume fraction of the  $Al_{11}RE_3$  phase and  $\alpha+\gamma$  eutectic was also presented. The hardness, impact strength, tensile strength as well as the yield strength of the alloy were examined in tests at room temperature. The examined experimental Mg-Al-RE-type magnesium alloy exhibited higher mechanical properties than the commercial AZ91 alloy (cast in the same conditions).

**Keywords:** Mg-Al-RE-type magnesium alloy, Microstructure, Mechanical properties

## 1. Introduction

Mg-Al-RE-type alloys (where RE denotes rare earth elements) are very attractive materials due to their low density and good mechanical properties, especially at elevated temperature. They are designed particularly for enhanced creep resistance [1-4]. The most economical solution is the production of alloys with a mixture of rare earth elements, although the influence of single elements (like cerium, neodymium, praseodymium or lanthanum) on the microstructure and various properties of Mg-Al-RE-type alloys have been also studied [5]. In these alloys, the main phase which is responsible for the properties of the final material is  $Al_{11}RE_3$  [5-8]. In alloys fabricated with didymium (i.e. a neodymium-rich mixture of rare earth elements), the main phase is identified on the basis of the

$Al_{11}Nd_3$  intermetallic compound, whereas in materials produced with cerium-rich mischmetal, it is identified by the  $Al_{11}Ce_3$  phase. Many studies have also focused on the thermal stability of this intermetallic compound, especially above 423 K and during creep tests [5]. The volume fraction of the  $Al_{11}RE_3$  phase depends on the chemical composition of the alloy, i.e. a reciprocal ratio of aluminium and rare earth elements. It should be added that the presence and volume fraction of the  $\gamma$  phase (precisely  $\alpha+\gamma$  eutectic) in the microstructure of these alloys also depends on this ratio. The  $\gamma$  phase (called sometimes  $\beta$  phase) is a typical structural constituent of Mg-Al-type alloys and has the stoichiometry of  $Mg_{17}Al_{12}$  (or  $Mg_{17}(Al, Zn)_{12}$  - in alloys from the Mg-Al-Zn-system) [8-10].

Among Mg-Al-RE alloys, commercial materials can be distinguished, such as the most popular AE42 or AE44 alloys, and many other alloys produced for specific applications (e.g. MRI



alloys) or for research purposes [5]. Most often, these alloys are fabricated by casting methods, in which single elements or different base alloys (like AM or AZ-type) are used. Mg-Al-RE-type alloys can also be cast by various methods, although significantly higher mechanical properties of these materials are obtained after using the high-pressure die casting (hpdc) method owing to the intensive reduction of size of structural constituents [2]. It should also be added that the mechanical properties of this type of alloys are very sensitive to the casting parameters, similar to all magnesium alloys. Additionally, various Mg-RE materials are also intensively investigated as the matrix alloys of metal matrix composites [11-14].

In the present paper, investigations of the microstructure and main mechanical properties of an experimental as-cast Mg-Al-RE-type alloy with a high weight fraction of aluminium and rare earth elements is presented. The results of the mechanical tests are compared with the results obtained for the commercial AZ91 alloy (cast under the same conditions).

## 2. Experimental procedures

The experimental magnesium alloy (called AEZ951 in this study) was fabricated on the basis of the commercial AZ91 alloy (cast under the same conditions for comparison) with 5.0 wt% rare earth elements (in the form of cerium-rich mischmetal with the chemical composition according to attestation: 54.8 wt% Ce, 23.8 wt% La, 16 wt% Nd, 5.4 wt% Pr, 0.16 wt% Fe and 0.19 wt% Mg). The alloy was produced in a resistance furnace equipped with a steel crucible under a protective atmosphere. The prepared alloy was gravity cast into a cold steel mould. In order to verify the elemental composition of the fabricated casts, an atomic absorption spectrometer, a Solar 939 (ATI Unicam, USA) was used. The obtained results of the chemical composition of the produced alloy are presented in Table 1.

Table 1.

Chemical composition of experimental AEZ951 alloy

Alloy	Chemical composition wt%*				
	Al <sup>1</sup>	Ce <sup>1</sup>	RE <sup>2</sup>	Zn <sup>3</sup>	Mn <sup>1</sup>
AEZ951	8.70	2.71	4.93	0.74	0.29

\* Mg rest; <sup>1</sup> spectrophotometric analysis; <sup>2</sup> calculation; <sup>3</sup> ASTM B93-94

The specimens for the microstructure investigations were prepared by a standard metallographic procedure and were etched in a 1% solution of HNO<sub>3</sub> in C<sub>2</sub>H<sub>5</sub>OH for about 60 s. The microstructures were observed using an Olympus GX51 light microscope with differential interface contrast and a JOEL-6610LV scanning electron microscope (SEM) equipped with an energy dispersive X-ray spectrometer (EDX). In order to determine the phase composition of the fabricated alloy, X-ray diffraction (XRD) analyses were carried out by means of a Bruker D8 Advance diffractometer with CuK<sub>α</sub> X-ray radiation. Reflexes from particular phases were identified according to ICDD PDF-4+ cards [15]. Additionally, the volume fraction of the main structural constituents was determined by the binarization of light microscopy micrographs from ten areas.

Tests of the mechanical properties of the fabricated alloy including hardness (HB), impact strength (IS), ultimate tensile strength (UTS) and yield strength (TYS) were carried out according to relevant ASTM standards. The Brinell hardness was determined using a steel ball with a diameter of 5 mm and a load of 2451 N. The impact strength was examined with a Charpy V hammer (150 J impact energy). Standard samples with a length of 55 mm and a cross section of 10 mm (V-notch with a depth of 2 mm) were used for the tests. A MTS-810 servohydraulic testing machine at room temperature with a strain rate of  $4 \times 10^{-4} \text{ s}^{-1}$  was employed in order to determine the ultimate tensile strength and tensile yield strength. The examinations were carried out on standard rod-like samples with a diameter of 8 mm (each test for three random samples).

## 3. Results and discussion

Fig. 1 shows a representative micrograph of the microstructure of the fabricated magnesium alloy, whereas the X-ray diffraction micrograph is presented in Fig. 2. The alloy consists of three main phases, i.e. an  $\alpha$ (Mg) solid solution (with a hexagonal closed-packed structure with unit cell parameters:  $a = 0.32092 \text{ nm}$ ,  $c = 0.52105 \text{ nm}$ ), Al<sub>11</sub>RE<sub>3</sub> and  $\gamma$  intermetallic compounds. Based on the Al<sub>11</sub>Ce<sub>3</sub> phase with the space group Immm ( $a = 0.4389 \text{ nm}$ ,  $b = 1.0072 \text{ nm}$  and  $c = 1.3011 \text{ nm}$  [15]) Al<sub>11</sub>RE<sub>3</sub> was identified. On the other hand, the  $\gamma$  phase was identified on the basis of the Mg<sub>17</sub>Al<sub>12</sub> intermetallic compound (I43m space group), although due to the chemical composition of the alloy the presence of zinc in the composition of this phase should be expected. In all magnesium alloys with aluminium, the  $\gamma$  phase occurs as a component of a fully or partially divorced eutectic with an  $\alpha$  phase. It is important to note that an Al<sub>10</sub>RE<sub>2</sub>Mn<sub>7</sub> intermetallic compound was also identified. This phase is formed owing to the low weight percentage of manganese in the chemical composition of the alloy and replaced the Al<sub>8</sub>Mn<sub>5</sub> phase, which is typical for Mg-Al-type alloys with manganese, such as the AM or AZ-series. Based on the ternary Al<sub>10</sub>Ce<sub>2</sub>Mn<sub>7</sub> phase with the R-3m space group ( $a = b = 0.9040 \text{ nm}$ ,  $c = 1.3170 \text{ nm}$  [15]) the Al<sub>10</sub>RE<sub>2</sub>Mn<sub>7</sub> phase was identified. It should also be noted that the Al<sub>2</sub>RE phase was not formed in the microstructure of the experimental alloy. This phase has often been observed in alloys with a lower weight percentage of aluminium or a high RE/Al ratio (close to or equal to 1) [5]. Because of the fine structural constituents, particular phases are better visible at higher magnification and using a scanning electron microscope. Fig. 3 presents SEM micrographs of the as-cast experimental AEZ951 magnesium alloy. Individual components of the microstructure were identified on the basis of their characteristic morphology and chemical composition obtained from EDX analyses. Fig. 3b presents exemplary results of the SEM+EDX investigations. Quantitative analyses of the presented microstructure revealed that the volume fraction of the Al<sub>11</sub>Ce<sub>3</sub> phase is 8% (standard deviation:  $\pm 0.4\%$ ), while the  $\alpha$ + $\gamma$  eutectic is 4% (standard deviation:  $\pm 0.9\%$ ). It should be noted that for the AZ91 alloy, cast under the same conditions, the volume fraction of the  $\alpha$ + $\gamma$  eutectic is about 15% (standard deviation:  $\pm 0.5\%$ ).

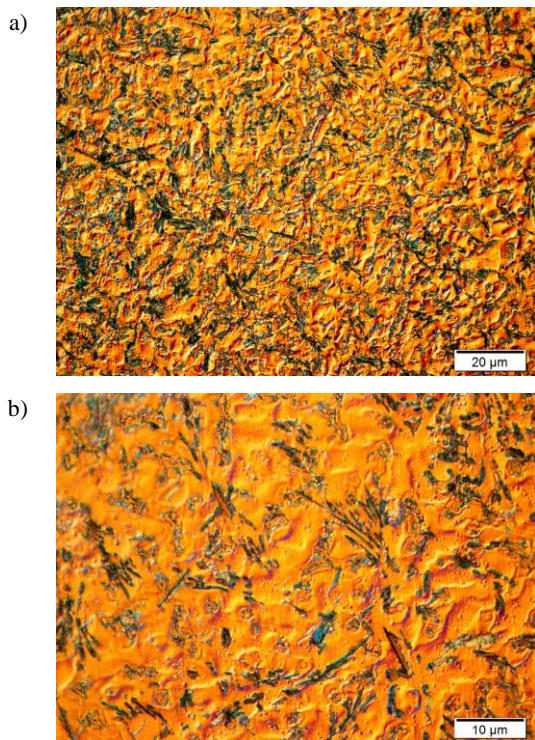


Fig. 1. Microstructure of as-cast experimental AEZ951 magnesium alloy; light microscopy with differential interface contrast

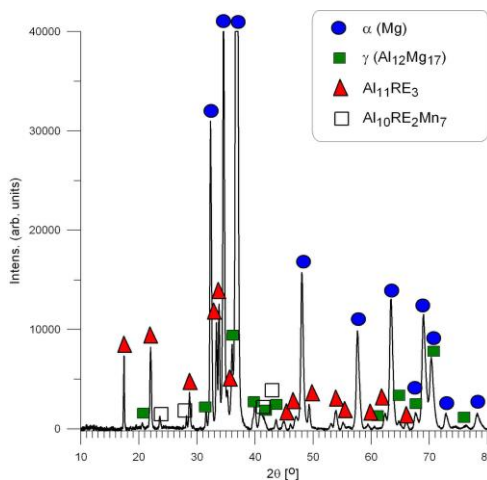


Fig. 2. X-ray diffraction pattern of as-cast experimental AEZ951 magnesium alloy

During solidification of the investigated alloy, the  $Al_{11}Ce_3$  phase forms at a higher temperature and consumes a significant volume fraction of aluminium. The  $\alpha+\gamma$  eutectic is formed at a lower temperature in the final stage of solidification (710 K) from the remaining aluminium located in the interdendritic regions formed as a result of fluctuation in the chemical composition during non-equilibrium solidification. It is obvious that some aluminium is also dissolved in the  $\alpha(Mg)$  solid solution but with a low mass fraction (i.e. 3.8 wt% - according to Point 1 in the Fig.

3b). It should also be noted that the mass fraction of manganese is low; therefore, the difference in the volume fraction of aluminium in the  $Al_{10}RE_2Mn_7$  intermetallic compound (in the experimental alloy) and in the  $Al_8Mn_5$  phase (in the AZ91 alloy) is not significant. The volume fraction of these phases is controlled mainly by the mass fraction of manganese in the chemical composition of the alloys.

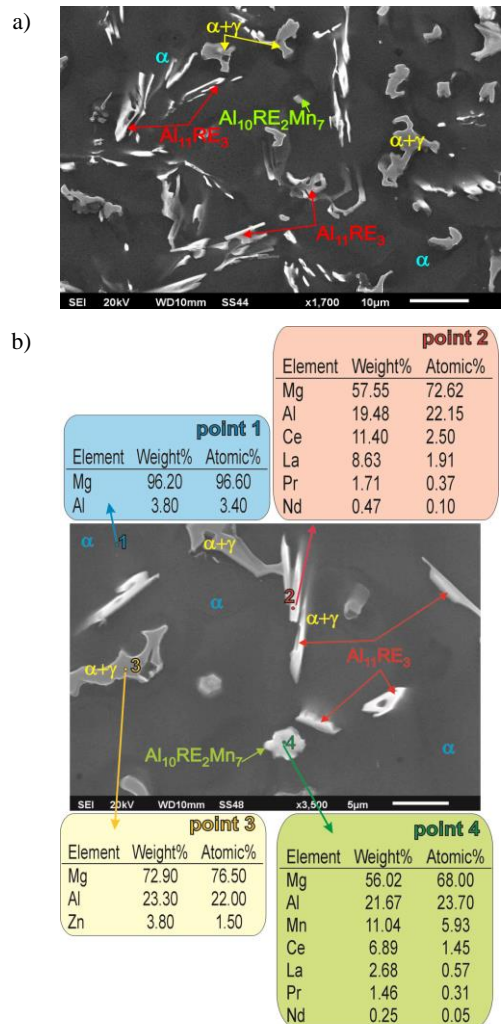


Fig. 3. SEM micrograph of as-cast experimental AEZ951 magnesium alloy with EDX results from designated points

The Brinell hardness of the experimental AEZ951 magnesium alloy was equal to 72 (standard deviation:  $\pm 0.8\%$ ), whereas the impact strength amounted to 2 J. For AZ91 the same parameters were 62 (standard deviation:  $\pm 1.2\%$ ) and also 2 J, respectively. The ultimate tensile strength and the ultimate yield strength at room temperature for the investigated magnesium alloy were equal: 183 MPa (standard deviation:  $\pm 8.3\%$ ) and 101 MPa (standard deviation:  $\pm 0.9\%$ ), respectively, while the same properties for the AZ91 alloy amounted to 125 MPa (standard deviation:  $\pm 3.5\%$ ) and 87 MPa (standard deviation:  $\pm 2.1\%$ ). The

presented results indicated that the influence of rare earth elements on the investigated properties at room temperature of the gravity cast alloy with 9 wt% aluminium is noticeable and positive. The  $Al_{11}RE_3$  phase with a plate-like morphology blocks the dislocation mobility; hence, the increase in mechanical properties is related to the amount of this structural constituent. It should also be noted that under the same casting parameters, Mg-Al-RE-type alloys always have a finer microstructure (with an intensive reduction in the size of the primary  $\alpha(Mg)$  solid solution dendrites) than Mg-Al-type alloys [5]. This factor also has a significant influence on the mechanical properties. On the other hand, the presented results revealed the same impact strength of the experimental AEZ951 and the commercial AZ91 magnesium alloy. It should be noted, however, that the brittle Al-RE-type intermetallic phases very often cause a slight decrease in the impact strength in Mg-Al-RE-type alloys. The negative influence of the increase in the volume fraction of the  $Al_{11}RE_3$  phase on the impact strength of alloys was presented in earlier studies for alloys with 5 wt% aluminium [2]. Therefore, the lack of a significant change in this property between the AZ91 and AEZ951 alloys should also be considered positive.

## 4. Conclusions

In the presented work, the experimental AEZ951 magnesium alloy designed on the basis of the AZ91 alloy was investigated. The main conclusions drawn are as follows:

1. The microstructure of the investigated alloy consists of an  $\alpha(Mg)$  solid solution and  $Al_{11}RE_3$ ,  $\gamma$  and  $Al_{10}RE_2Mn_7$  intermetallic compounds.
2. A high weight fraction of rare earth elements in the chemical composition of the alloy results in a large volume fraction of the  $Al_{11}RE_3$  phase and a small volume fraction of the  $\alpha+\gamma$  eutectic.
3. The fabricated experimental alloy has higher mechanical properties (HB, UTS, TYS) at room temperature than the commercial AZ91 alloy, (cast under the same conditions); nevertheless, the impact strength remains at the same level.

## References

- [1] Lee, S.G., Patel, G.R., Gokhale, A.M., Sareeranganathan, A. & Horstemeyer, M.F. (2006). Quantitative fractographic analysis of variability in the tensile ductility of high-pressure die-cast AE44 Mg-alloy. *Materials Science Engineering A*. 427(1-2), 255-262. DOI: 10.1016/j.msea.2006.04.108.
- [2] Braszczyńska-Malik, K. & Malik, M.A. (2020). Impact strength of AE-type alloys high pressure die castings. *Archives of Foundry Engineering*. 20(3), 5-8. DOI:10.24425/afe.2020.133321.
- [3] Yang, Q., Guan, K., Li, B., Lv S., Meng F., Sun W., Zhang Y., Liu, X. & Meng, J. (2017). Microstructural characterizations on Mn-containing intermetallic phases in a high-pressure die-casting Mg-4Al-4RE-0.3Mn alloy. *Materials Characterization*. 132, 381-387. <https://doi.org/10.1016/j.matchar.2017.08.032>.
- [4] Yang, Q., Lv, SH., Meng, FZ., Guan, K., Li, B.-S., Zhang, X-H., Zhang, J.-Q., Liu X.-J. & Meng, J. (2019). Detailed structures and formation mechanisms of well-known  $Al_{10}RE_2Mn_7$  phase in die-cast Mg-4Al-4RE-0.3Mn Alloy. *Acta Metallurgica Sinica (English Letters)*. 32, 178-186. <https://doi.org/10.1007/s40195-018-0819-0>.
- [5] Braszczyńska-Malik, K.N. & Grzybowska, A. (2016). Influence of phase composition on microstructure and properties of Mg-5Al-0.4Mn-xRE (x = 0, 3 and 5 wt.%) alloys. *Materials Characterization*. 115, 14-22. <https://doi.org/10.1016/j.matchar.2016.03.014>
- [6] Zhou, W., Li, Z., Li, D., Qin, M. & Zeng, X. (2022). Solidification microstructure evolution in LA42 Mg alloy under various cooling rates. *Journal of Materials Science*. 57, 11411-11429. <https://doi.org/10.1007/s10853-022-07330-5>
- [7] Cai, H., Wang, Z., Liu, L., Li, Y., Xing, F. & Guo F. (2022). Formation sequence of compounds in AZ91-0.9Ce alloy and its role in fracture process. *Advanced Engineering Materials*. 24(7), 2101411. <https://doi.org/10.1002/adem.202101411>.
- [8] Braszczyńska-Malik, K.N. (2014). Some mechanical properties of experimental Mg-Al-Mn-RE alloy. *Archives of Foundry Engineering*. 14(1), 13-16. DOI: 10.2478/afe-2014-0003.
- [9] Yang, Q., Guan, K., Li, B., Lv, S., Meng, F., Sun, W., Zhang, Y., Liu, X. & Meng, J. (2017). Microstructural characterizations on Mn-containing intermetallic phases in a high-pressure die-casting Mg-4Al-4RE-0.3Mn alloy. *Materials Characterization*. 132, 381-387. <https://doi.org/10.1016/j.matchar.2017.08.032>.
- [10] Zhou, W., Li, Z., Li, D., Qin, M. & Zeng X. (2022). Solidification microstructure evolution in LA42 Mg alloy under various cooling rates. *Journal of Materials Science*. 57, 11411-11429. <https://doi.org/10.1007/s10853-022-07330-5>.
- [11] Braszczyńska, K.N. (2003). Contribution of SiC particles to the formation of the structure of Mg-3 wt.% RE cast composites. *Zeitschrift für Metallkunde*. 94, 144-148. <https://doi.org/10.3139/ijmr-2003-0028>.
- [12] Li, L., Li, D., Zeng, X., Luo, A.A., Hu, B., Sachdev, A. K., Gu, L. & Ding, W. (2020). Microstructural evolution of Mg-Al-RE alloy reinforced with alumina fibers. *Journal of Magnesium Alloys*. 8(3), 565-577. <https://doi.org/10.1016/j.jma.2019.07.012>
- [13] Braszczyńska-Malik, K. & Przełoczyńska, E. (2017). The influence of Ti particles on microstructure and mechanical properties of Mg-5Al-5RE matrix alloy composite. *Journal of Alloys and Compounds*. 728, 600-606. <https://doi.org/10.1016/j.jallcom.2017.08.177>.
- [14] Tang, B., Li, J., Wang, Y., Luo, H., Ye, J., Chen, X., Chen, X., Zheng, K. & Pan, F. (2022). Mechanical properties and microstructural characteristics of Ti/WE43 composites. *Vacuum*. 206, 111534. <https://doi.org/10.1016/j.vacuum.2022.111534>
- [15] Powder Diffraction File, PDF-4+, International Centre for Diffraction Data (ICDD), Pennsylvania, USA, 2014.